Photorefractive recording by a special mechanism in planar LiNbO₃ waveguides

D. Kip, F. Rickermann, and E. Krätzig

Fachbereich Physik, Universität Osnabrück, 49069 Osnabrück, Germany

Recording of holographic gratings in z-cut LiNbO₃ waveguides with extraordinarily (TM) polarized light is demonstrated. In this geometry, photovoltaic currents perpendicular to the guiding layer and the grating vector set up space-charge fields. The mechanism has no equivalent in bulk material.

In optical waveguides the high light intensities that are readily obtained with moderate input powers permit the observation of large photorefractive effects. Together with the possibility of low-voltage beam modulation through surface electrodes, this has led to the development of several nonlinear-optical devices, e.g., switches, sensors, and memory cells, based on photorefractive waveguides.[1,2]

Because of the small dimensions (a few micrometers) of the guiding structure, light propagation is allowed only for a limited number of modes. As a result, planar waveguides show several scattering and coupling processes that have no equivalent in bulk crystals. Examples are parametric intermode scattering in LiNbO₃ waveguides[3] and the coupling of orthogonally polarized waves.[4]

In this Letter we investigate the writing of holographic gratings in planar z-cut LiNbO₃ waveguides with two extraordinarily (TM) polarized modes. In this geometry, photovoltaic currents in the direction normal to the waveguide surface are excited, while the grating vector lies in the waveguiding layer nearly perpendicular to the propagation direction. Decisive for the formation of a grating is the small thickness of the waveguiding layer, which has to be comparable with the grating period. In the bulk material, space-charge fields may be set up by diffusion of charge carriers, but there is no active electro-optic tensor element for read-out in such a configuration.

We consider the interaction of two extraordinarily (TM) polarized waves traveling at a small angle $\pm\theta$ with respect to the x axis in a z-cut LiNbO₃ waveguide (Fig. 1). The dominating part of the electric field oscillates in the z direction, whereas the longitudinal component is very small. Neglecting absorption, we can write the interference pattern $|E|^2(y,z)$ of the two waves in the form

$$|E|^2(y,z) = |A|^2|U(z)|^2$$
$$\times \ [1 + m\cos(\mathbf{k} \cdot \mathbf{y})], \qquad (1)$$

where A and U are the amplitude and the mode function, respectively, m is the modulation, $\mathbf{k}$ is the grating vector with $|\mathbf{k}| = 4\pi n_{\text{eff}}\sin\theta/\lambda$, n_{eff} is the effective refractive index, λ is the wavelength of light in vacuum, and θ is the half writing angle.

In photorefractive crystals, electrons or holes can be excited by inhomogeneous illumination and migrate under the influence of external, diffusion,[5] pyroelectric,[6] or photovoltaic[7] fields. Especially for Fe- and Cu-doped LiNbO₃ crystals, redistribution of photoexcited charge carriers by the photovoltaic effect is the dominating process for the formation of holographic gratings. The polarization-dependent current density is given by[8]

$$j_k^{\text{ph}} = \sum_{l,m} \beta_{k,lm}E_l{}^*E_m, \qquad (2)$$

with $\hat{\beta}$ for the photovoltaic tensor and $E_{l,m}$ for the light field.

In the considered configuration the light pattern $|\mathbf{E}|^2$ modulated in the y direction excites a current of density $j_3^{\text{ph}} = \beta_{3,33}|E_3|^2$ along the z axis (Fig. 2). Because of this photovoltaic current, charge carriers are separated perpendicular to the waveguiding layer. A space-charge field $\mathbf{E}^{\text{sc}}$ builds up:

$$\mathbf{E}^{\text{sc}} = \hat{\sigma}^{-1}\mathbf{j}^{\text{drift}}, \qquad (3)$$

with $\mathbf{j}^{\text{drift}}$ for the drift current density caused by the electric field. Here photoconductivity $\hat{\sigma}^{\text{spec}}I$ ($\hat{\sigma}^{\text{spec}}$ is the specific photoconductivity) and dark conductivity $\hat{\sigma}^d$ contribute to the total conductivity $\hat{\sigma} = \hat{\sigma}^d + \hat{\sigma}^{\text{spec}}I$.

The space-charge field in the z direction has a dc component and an ac part modulated with $\cos(\mathbf{k} \cdot \mathbf{y})$ (see Fig. 2). However, in the y direction there is no dc offset of the electric field. In the maximum and minimum positions of the photovoltaic current distribution $j_3^{\text{ph}}(y)$ the space-charge field component E_2^{sc} is zero, and the modulated part can be described by a sin function. According to Eq. (1) we have no dependence of the space-charge field in the x direction. Altogether, the space-charge field can be written in the form

$$\mathbf{E}^{\text{sc}}(y,z) = [0, A_2^{\text{sc}(1)}(z)\sin(\mathbf{k} \cdot \mathbf{y}),$$
$$A_3^{\text{sc}(0)}(z) + A_3^{\text{sc}(1)}(z)\cos(\mathbf{k} \cdot \mathbf{y})]. \qquad (4)$$
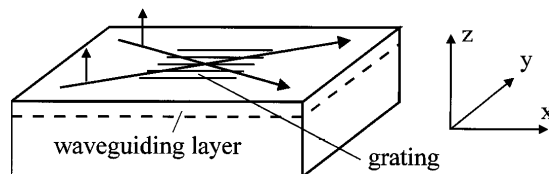
Fig. 1. Configuration for writing holographic gratings in z-cut LiNbO₃ waveguides by using extraordinarily polarized light. The propagation directions and polarizations of the interacting waves are shown by arrows.
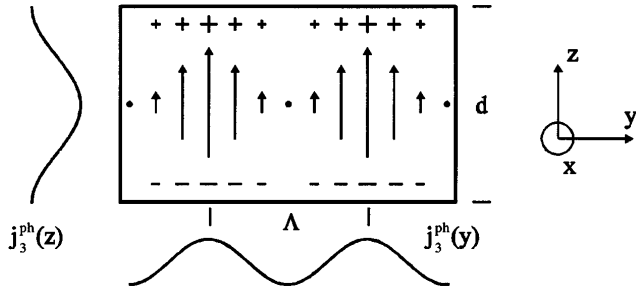
Fig. 2. Schematic representation of the photovoltaic current density $j_3^{ph}(y, z)$ in the yz plane of a z-cut waveguide. Here $\Lambda = 2\pi/|\mathbf{k}|$ is the grating period and d is the effective waveguide thickness. The arrows illustrate the current density for the lowest-mode TM_0.

Here $A_3^{sc(0)}$ is the amplitude of the dc field component in the z direction and $A_2^{sc(1)}$ and $A_3^{sc(1)}$ are the ac components modulated with $\sin(\mathbf{k} \cdot \mathbf{y})$ and $\cos(\mathbf{k} \cdot \mathbf{y})$, respectively.

By inserting the equations for the photovoltaic current and the space-charge field into the continuity equation and using the Maxwell equations $\text{div}(\mathbf{j}^{ph} + \mathbf{j}^{drift}) = 0$ and $\text{rot}(\mathbf{E}^{sc}) = 0$, we obtain two differential equations for the dc and ac component of the space charge field in the z direction:

$$\frac{d}{dz} A_3^{sc(0)}(z) = \frac{|A|^2 [d|U(z)|^2/dz]}{|A|^2 |U(z)|^2 + \sigma_{33}^d/\sigma_{33}^{spec}}$$
$$\times \left[A_3^{sc(0)}(z) + \frac{\beta_{3,33}}{\sigma_{33}^{spec}} \right], \qquad (5)$$

$$\frac{d^2}{dz^2} A_3^{sc(1)}(z) = k^2 A_3^{sc(1)}(z)$$
$$- \frac{d}{dz} \left[\frac{m|A|^2 |U(z)|^2}{|A|^2 |U(z)|^2 + \sigma_{33}^d/\sigma_{33}^{spec}} \frac{d}{dz} A_3^{sc(0)}(z) \right]$$
$$- \frac{d}{dz} \left(\left\{ \frac{|A|^2 [d|U(z)|^2/dz]}{|A|^2 |U(z)|^2 + \sigma_{33}^d/\sigma_{33}^{spec}} \right\} \right.$$
$$\left. \times \left[\frac{m\beta_{3,33}}{\sigma_{33}^{spec}} + m A_3^{sc(0)}(z) + A_3^{sc(1)}(z) \right] \right). \quad (6)$$

By means of the electro-optic effect, $\Delta n_e = -0.5 n_e^3 r_{33,3} E_3^{sc}$, the space-charge field modulates the extraordinary refractive index and produces a grating in phase with the intensity distribution. Here $r_{33,3}$ is the relevant electro-optic tensor element. The space-charge field in the y direction, $A_2^{sc(1)} \sin(\mathbf{k} \cdot \mathbf{y})$, does not lead to a coupling of the two extraordinarily polarized waves because $r_{33,2} = 0$ in crystals with symmetry $3m$.

The mode functions U of the guided modes can be calculated for a given refractive-index profile by integration of the mode equations. With the experimental parameters A, σ_{33}^{spec}, σ_{33}^d, and $\beta_{3,33}$, Eqs. (5) and (6) for the components of the space-charge field can be solved. The ratio $\sigma_{33}^d/\sigma_{33}^{spec}$ describes the intensity dependence of the space-charge field, while the parameter $\beta_{3,33}$ scales only with the magnitude of the electric field.

As an example, Fig. 3 shows the space-charge field distribution $E_3^{sc} = A_3^{sc(0)} + A_3^{sc(1)}$ for a z-cut waveguide in the yz plane. Two TM_1 modes of equal intensity intersect at an angle of $2\theta = 4.4°$ (grating period 3 μm). We use the refractive-index profile of the waveguide $Ti-z-Fe$ (Gaussian profile with depth $\rho = 8$ μm, $\Delta n_e = 0.02$, $n_e^0 = 2.248$) and measured values for σ_{33}^d, σ_{33}^{spec}, and amplitude $|A|^2$ (see the caption to Fig. 3). The photovoltaic constant $\beta_{3,33}$ is proportional to the concentration of filled traps (Fe^{2+}, Cu^+) and was not measured. We use a value that was obtained for oxidized $LiNbO_3$:Fe (0.1 wt. % Fe_2O_3) bulk crystals.

The possibility of recording holographic gratings in z-cut waveguides by using extraordinarily polarized light has been proved experimentally in different $LiNbO_3$ waveguides. Samples have been prepared by Ti indiffusion (80-nm Ti layer indiffused for 24 h at 1000 °C in an Ar atmosphere) followed by either Fe or Cu indiffusion (80-nm Fe or Cu layer indiffused for 18 h at 1000 °C in an O_2 atmosphere). For comparison, waveguides with the same parameters as above were also fabricated in y-cut $LiNbO_3$. Furthermore, we prepared waveguides by using a combined proton and Cu exchange in z-cut samples.[9]

For writing holographic gratings, two beams of an Ar-ion laser ($\lambda = 514.5$ nm) with equal intensity are coupled into and out of the waveguide with rutile prisms. During the buildup of a refractive-index grating, we measure the diffraction efficiency as a function of time by blocking one of the beams for a short time (50 ms) and measuring the ratio of diffracted light and total light intensity of the outcoupled beams. When saturation is reached, one of the beams is switched off, and the diffracted light intensity indicates the decay of the grating during readout.

Table 1 summarizes the results of the holographic investigations. The values are obtained with either TM_1 or TE_1 modes, $2\theta = 4.4°$, and an interaction length of 2.5 mm. For z-cut waveguides, η_{TM} is the maximum diffraction efficiency when extraordinarily (TM) polarized light is used and η_{TE} is that for ordinary (TE) polarization.

In the three different z-cut waveguides ($Ti-z-Fe$, $Ti-z-Cu$, and $PE-z-Cu$), large diffraction efficiencies ranging from 0.05 to nearly 1 are reached by extraor-
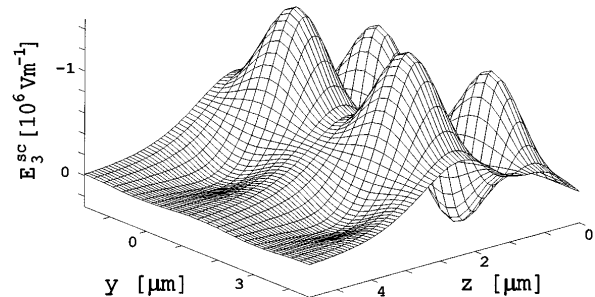
Fig. 3. Calculated distribution E_3^{sc} of the z component of the space-charge field for a z-cut waveguide in the yz plane. Two TM_1 modes propagate under an angle $\theta = \pm 2.2°$ with respect to the x axis. The space-charge field is a solution of Eqs. (7) and (8) with $\sigma_{33}^d = 4 \times 10^{-11}$ $A V^{-1} m^{-1}$, $\sigma_{33}^{spec} = 2 \times 10^{-17}$ $m V^{-2}$, $|A|^2 = 10^5$ $W m^{-2}$, and $\beta_{3,33} = 10^{-9}$ V^{-1}.

Table 1. Experimental Results for Diffraction Efficiency η (Obtained with Two Either TM$_1$ or TE$_1$ Modes) of Holographic Gratings Written up to Saturation in Different z-Cut LiNbO$_3$ Waveguides

Waveguide	Cut	Doping	η_{TM}	η_{TE}
Ti–z–Fe	z	Fe	0.089	0.021
Ti–z–Cu	z	Cu	0.047	0.014
PE–z–Cu	z	Cu	0.95	–
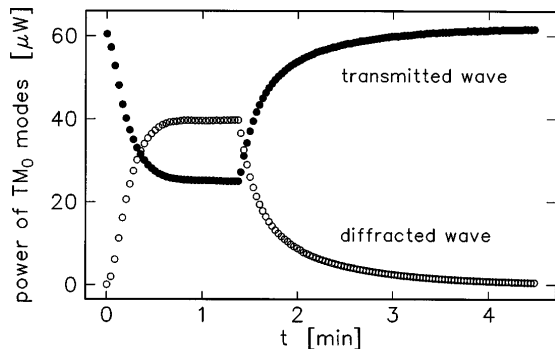
Fig. 4. Time evolution of writing ($0 < t < 85$ s) and reading ($t \geq 85$ s) of a holographic grating in a z-cut LiNbO$_3$ waveguide (PE–z–Cu) with two TM$_0$ modes. After 60 s a steady-state diffraction efficiency of 0.65 is reached. With an input power of 200 μW for each wave and an absorption of ~0.5 mm^{-1}, photoconductivity exceeds dark conductivity by 1 order of magnitude. Note that for the writing process the intensity in the waveguide is twice that of the reading process, leading to a smaller time constant for the buildup of the grating.

dinary (TM) polarization. Figure 4 shows as an example the writing and reading dynamics of a grating in a proton-exchanged (PE) Cu-doped z-cut LiNbO$_3$ waveguide. Here a steady-state diffraction efficiency of 0.65 for TM$_0$ modes (0.95 for TM$_1$ modes; Table 1) is reached after 60 s. These high values clearly demonstrate the advantages of the combined proton and Cu exchange. No energy coupling is observed during recording, showing that the refractive-index grating is in phase with the intensity pattern.

When using ordinarily (TE) polarized light in z-cut samples, we have a mixture of two writing processes. One grating is written because of photovoltaic currents propagating normally to the waveguiding layer as described above but excited by $\beta_{3,22}$ that is comparable in magnitude with $\beta_{3,33}$.[10] Furthermore, photovoltaic currents are excited by $\beta_{2,22}$ in the direction of the grating vector as in a common writing geom-

etry. So the total diffraction efficiency for this geometry is larger than the value expected from the relation $\eta_{\mathrm{TE}} \approx (n_o^3 r_{11,3})^2 / n_e^3 r_{33,3})^2 \eta_{\mathrm{TM}} \approx 0.14 \eta_{\mathrm{TM}}$. In proton-exchanged waveguides light is guided only under the extraordinary refractive index.[11]

In y-cut waveguides gratings are written in a normal configuration in which the photovoltaic current and the grating vector are in the same direction. In these samples we measure values from 4% to 7% for the diffraction efficiency that have approximately the same magnitude as in indiffused z-cut waveguides. This comparison shows that the mechanism for writing holographic gratings in z-cut samples with photovoltaic currents perpendicular to the waveguiding layer is effective similarly to that in a normal geometry.

In summary, we have described a new method to write holographic gratings in planar z-cut waveguides, using extraordinarily polarized light. There is no equivalent mechanism in the bulk material. For proton-exchanged LiNbO$_3$ and LiTaO$_3$ waveguides in z-cut substrates, where only extraordinarily polarized light is guided, this is the only possible mechanism for recording refractive-index gratings.

References

1. V. E. Wood, P. J. Cressman, R. L. Holman, and C. M. Verber, in *Photorefractive Materials and Their Applications II,* Vol. 61 of Topics in Applied Physics, P. Günter and J.-P. Huignard, eds. (Springer-Verlag, Berlin, 1989), pp. 45–100.
2. A. Donaldson, J. Phys. D **24,** 785 (1991).
3. A. D. Novikov, S. G. Odoulov, V. M. Shandarov, E. S. Shandarov, and S. M. Shandarov, J. Opt. Soc. Am. B **8,** 1298 (1991).
4. D. Kip and E. Krätzig, Opt. Lett. **17,** 1563 (1992).
5. D. L. Staebler and J. J. Amodei, J. Appl. Phys. **43,** 1042 (1972).
6. K. Buse, J. Opt. Soc. Am. B **10,** 1266 (1993).
7. A. M. Glass, D. von der Linde, and T. J. Negran, Appl. Phys. Lett. **25,** 255 (1974).
8. V. I. Belinicher and B. Sturman, Sov. Phys. Usp. **23,** 199 (1980).
9. S. M. Kostritskii and O. M. Kolesnikov, J. Opt. Soc. Am. B **11,** 1674 (1994).
10. H. G. Festl, P. Hertel, E. Krätzig, and R. von Baltz, Phys. Status Solidi B **113,** 157 (1982).
11. V. A. Gan'shin and Y. N. Korkishko, Phys. Status Solidi A **119,** 11 (1990).